INTERFACE

Auditory mechanics in a bush-cricket: direct evidence of dual sound inputs in the pressure difference receiver.

Journal:	*Journal of the Royal Society Interface*
Manuscript ID	rsif-2016-0560.R1
Article Type:	Research
Date Submitted by the Author:	n/a
Complete List of Authors:	Jonsson, Thorin; University of Lincoln, School of Life Sciences; University of Bristol, School of Biological Sciences Montealegre-Z , Fernando ; University of Lincoln, School of Life Sciences Soulsbury, Carl; University of Lincoln, School of Life Sciences Robson Brown, Katharine; University of Bristol, Department of Archaeology and Anthropology Robert, Daniel; University of Bristol, School of Biological Sciences
Categories:	Life Sciences - Physics interface
Subject:	Biomechanics < CROSS-DISCIPLINARY SCIENCES, Biophysics < CROSS-DISCIPLINARY SCIENCES
Keywords:	tympanum, sound processing, bush-cricket, katydid, sound propagation, acoustic trachea

Auditory mechanics in a bush-cricket: direct evidence of dual sound inputs in the pressure difference receiver.

Thorin Jonsson [1, 3, †], Fernando Montealegre-Z. [1,*, †], Carl Soulsbury [1], Kate A. Robson Brown [2] and Daniel Robert [3]

[1] School of Life Sciences, Joseph Banks Laboratories, Green Lane, Lincoln, LN6 7DL, UK

[2] Imaging Lab, Archaeology and Anthropology, University of Bristol, 43 Woodland Road, Bristol, BS8 1UG, UK

[3] School of Biological Sciences, University of Bristol, 24 Tyndall Avenue, Bristol, BS8 1TQ, UK

*Author for correspondence (fmontealegrez@lincoln.ac.uk)

†These authors have contributed equally to this work

Short running title: "pressure difference auditory mechanics"

Summary

The ear of the bush-cricket *Copiphora gorgonensis* consists of a system of paired eardrums (tympana) on each foreleg. In these insects, the ear is backed by an air-filled tube, the acoustic trachea (AT), which transfers sound from the prothoracic acoustic spiracle to the internal side of the eardrums. Both surfaces of the eardrums of this auditory system are exposed to sound, making it a directionally sensitive pressure-difference receiver. A key feature of the AT is its capacity to reduce the velocity of sound propagation and alter the acoustic driving forces at the tympanum. The mechanism responsible for reduction in sound velocity in the AT remains elusive, yet it is deemed to depend on adiabatic or isothermal conditions. To investigate the biophysics of such multiple input ears, we used micro-scanning laser Doppler vibrometry and micro-computed X-ray tomography. We measured the velocity of sound propagation in the acoustic trachea, the transmission gains across auditory frequencies, and the time-resolved mechanical dynamics of the tympanal membranes in *Copiphora gorgonensis*. Tracheal sound transmission generates a gain of ~15 dB SPL, and a propagation velocity of *ca*. 255 m/s, a ~25% reduction from free field propagation. Modelling tracheal acoustic behaviour that accounts for thermal and viscous effects, we conclude that reduction in sound velocity within the acoustic trachea can be explained, amongst others, by heat exchange between the sound wave and the tracheal walls.

Key words: Tympanum, sound processing, katydid, bush-cricket, sound propagation, acoustic trachea

1. INTRODUCTION

For the majority of animals endowed with tympanal ears, incident pressure waves act on the external surface area of thin and compliant tympanal membranes. Bush-crickets (Orthoptera, Ensifera, Tettigoniidaep have pairs of eardrums for each ear, located within their forelegs. Instead of acting only on the external surface of the eardrums membranes, sound pressure acts on both the external and internal surfaces [1-.I. The internal acoustic input is enhanced by an air-filled tube, the acoustic trachea (ATp, that conveys sound from an opening on the side of the thorax (the acoustic spiraclep to the internal side of the eardrums [1-A, 8]. The AT is a gradually narrowing pipe that extends forwards from the thorax through into the fore femoral cavity until it reaches the femoro-tibial joint (the kneep, whereupon it enters the tibia and divides into two branches, an anterior feeding the anterior tympanal membrane (ATMpand a posterior branch connected with the posterior tympanal membrane (PTMp(see figure 1 for relative position of the tympanap[7-9I. Each tracheal branch leads to one tympanal membrane, and the dorsal part of the anterior branch harbours the ear mechanoreceptors (known as the *crista acustica*, CAp[10-12]. Dorsal to this area, between the two tympana on both sides of the tibia, lies the auditory vesicle, a fluid-filled cavity that encapsulates the CA [13]. Both tracheal divisions merge again below the tympanal membranes where the trachea narrows and ends right beneath the ear [9]. Each eardrum is placed against the outer surfaces of these tracheal divisions, creating the only place in the system where both sides of the tracheal wall are coupled to the outside air. Hence, both internal and external surfaces of the tympanal membranes are readily driven by sound waves travelling through the AT and by sound waves reaching the membrane externally.

It is broadly accepted that the AT is the main acoustic input of the ear of many Tettigoniidae species [2, 7, 14-17]. However, for the subfamily Pseudophyllinae (a large group with some 1000 species describedp the acoustic spiracle is reduced (a character used as diagnostic for this subfamilypand the bulla is replaced by a small chamber [18-20I and in some species the AT forms a large U-shape bend at the bulla site [6]. Although poorly understood, in Pseudophyllinae, the AT is unlikely to be the main acoustic input, and some authors suggest that the tympanal slits might play important role as waveguides [18, 20].

It is also agreed that in some species, the AT looks and functions like an exponential horn, increasing the magnitude of sound pressure acting on the internal side of the tympanal membranes [1, 5, 7, 14]. This gain-enhancing role is associated with the size of the spiracular opening and its associated bulla [5, 21]. The enhancement of the internal pressure acting on the back surface of the tympanal membranes is deemed to provide this auditory system with directional sensitivity (see below) [22, 23]. Some researchers argue that this exponential horn exhibits high-pass, high-gain characteristic to provide a broadband response necessary for acoustic reception [7].

The AT is thought to play a vital role in the formation of the pressure difference mechanism. A pressure difference receiver relies on the interference of sound waves at either surface of the tympanal membranes [23-25]. The internal sound pressure of sound waves travelling in the AT, undergoes different degrees of attenuation or amplification and some phase shift as a result of alterations in propagation velocity [23]. Phase shifts are produced because pressure waves push the tympanic membranes externally and internally, but also by differences in the time of arrival of sound waves on both surfaces caused by alterations in propagation velocity inside the AT. These changes in the propagation velocity result from the fact that the AT seems to impose resistance to sound propagation [24], effectively slowing down sound travelling through the AT compared to the sound waves travelling in the surrounding air and reaching the external side of the tympanum [4, 5, 26]. This time delay has been observed as a gradual change in the phase of the tympanal membrane vibrations and is particularly prominent at high frequencies [5]. The internal sound propagation can also be measured in the time domain when the ear is stimulated with pure-tone pulses. The impulse mechanical response should therefore exhibit two distinct vibrational events, which reveal the sound wave arriving twice at the tympanum, once externally and once internally. The difference in time lag appears to depend on leg position with respect to the sound source [4]. In summary, in a pressure difference receiver, a combination of both phase shift and amplitude difference is likely to take place, and to affect the ipsilateral and contralateral ears differentially [4, 23, 26].

Researchers have had differing opinions about the AT, its role in a pressure difference receiver ear and its effect on sound propagation. Discrepancies on the AT/pressure difference receiver ear might have arisen from different approaches, and techniques used over time (some invasive and deemed less appropriate [5, 7]), and from using different species, most of which communicate with broadband calls. Low propagation velocities of sound inside the AT (about 75% of sound velocity in air) are well documented in two species of field crickets [4, 25]. Previous studies provided clear evidence that sound propagation velocity is reduced within the AT of bush-crickets [27]. Yet, to date, the biophysical mechanisms of sound propagation within the AT, its potential dimorphism, its effects on spectral auditory sensitivity and on auditory mechanics remain elusive.

Here, we study *Copiphora gorgonensis* (Conocephalinae, Copiphorini), a neotropical bush-cricket species that communicates by producing sharply-narrow-band pure-tone calls with a carrier frequency centred at 23 kHz [28]. Like most Conocephalinae, males and females possess large acoustic bullae and narrow tracheae [13, 29], suggesting that the acoustic trachea might function as an exponential horn [1], therefore enhancing the internal pressure driving the tympanal membrane. If this is the case, vibrations of the tympanal membranes of individuals placed in the acoustic free field should show pressure and temporal differences produced by pressure waves acting on both sides of the tympana. Our hypothesis is that the internal sound input is significantly delayed compared to the sound wave following the external pathway to the tympanal membranes.

Following on our previous work [13], we also test the hypothesis that the ear of *C. gorgonensis* works as a pressure difference receiver that is effective over a broad range of frequencies.

Using micro-scanning laser Doppler vibrometry (LDV), micro-computed tomography (μ-CT), and an experimental platform permitting the controlled acoustic isolation of both internal and external inputs, we performed rigorous measurements of tympanal vibrations to quantify acoustic gain, temporal delay and spectral characteristics of sound propagation in the AT.

Our results demonstrate that the ear of *C. gorgonensis* functions as a pressure difference receiver. We show that internal sound input through the acoustic trachea is significantly delayed due to a 25% reduction in the propagation velocity of sound. This tracheal input also contributes a nearly fourfold gain as compared to the external input. The gain and propagation velocity are comparable to those found in other Orthoptera. The possible mechanisms at work in acoustic trachea responsible for the decrease in propagation velocity are discussed.

2. METHODS

2.1. Experimental animals

We used 21 *Copiphora gorgonensis* individuals (10 males, 11 females). This species is endemic to the island of Gorgona, Colombia, located off the south-western Colombian Pacific coast. Males call females in the low ultrasonic range using a pure-tone, short-duration pulse (8 ms) at 23 kHz [28]. Specimens were collected as nymphs in their natural habitat and maintained in captivity in cages at 25 °C, LD 11h: 23h and 70% RH, where they were fed on a mix of pollen and dry cat food until they reached adulthood.

2.2. Morphological studies of the acoustic trachea

The anatomy of the bush-cricket ear and the AT was examined using X-ray μ-computed tomography (μ-CT) and 3D reconstruction using standard biomedical imaging software following the protocols of Montealegre-Z et al. [13]. Four specimens (two males and two females) were scanned with a Bruker SkyScan 1272 (Bruker microCT, Kontich, Belgium) at 100 kV, 36 μA and with a 0.5 mm thick aluminium filter, resulting in a voxel size of 11 μm. Reconstruction and automated measurements of acoustic tracheae were carried out with Amira (v. 5.4, VSG, Berlin, Germany) and results further processed in Matlab (R2014a, The MathWorks, Inc., Natick, MA, USA). In addition, tracheal lengths of 20 individual (9 males and 11 females) were measured by inserting a thin human hair from the spiracle to the middle of the tympanal area. The insertion of the hair could be easily monitored visually through the semi-transparent leg cuticle and tympanal membranes.

2.3. Induction of tympanal vibration

Tympanal vibration in response to sound was studied using two different approaches: 1) Both surfaces of the tympanal membranes were exposed to sound by placing the specimen in the acoustic free field, and 2) the effect of multiple sound pathways was studied by generating internal and external sound inputs independent of each other.

1) The specimen was mounted in a bespoke holder and placed in the acoustic free field. The holder consists of a movable plate (with copper wires to secure the legs) screwed on an elbowed arm (for more details see Montealegre-Z et al. [13]). The forelegs were oriented forwards, in a position akin to the bush-cricket standing on a leaf. The holder was solidly tethered on a vibration isolation air table holding a LDV (Polytec PSV-300-F; Waldbronn, Germany). A loudspeaker (ACR, FT 17H, Fostex, Tokyo, Japan; or an ESS AMT-1, ESS Laboratory, Inc., Sacramento, CA, USA) was positioned 30 cm away, ipsilateral at 90° with respect to the body axis of the animal, playing periodic chirps in the range of 1-50 kHz. Computer controlled correction of the acoustic stimulus was used to maintain constant amplitude levels (60±1.5 dB SPL, re 20 µPa) at the tympanum across the whole frequency range. Broadband signals were generated at 512 kHz by the LDV internal data acquisition board (National Instruments PCI-4451; Austin, TX, USA), amplified (TAFE570; Sony, Tokyo, Japan) and passed to the loudspeaker. The velocity of the tympanal membrane vibrations was measured using the LDV with an OFV-056 scanning head fitted with a close-up attachment (Polytec; Waldbronn, Germany). Tympanal vibrations were analysed by simultaneously recording the vibration velocity of the tympanum, and the sound stimulus amplitude and frequency at the tympanum and at the spiracle entrance. Data quality was assessed using coherence for each data point [30]. Data were considered of sufficient quality when coherence exceeded 80%.

All sound pressure measurements were carried out with two 1/8" precision pressure microphones (Bruel & Kjaer, 4138; Nærum, Denmark) and a preamplifier (Bruel & Kjaer, 2633). The microphones were calibrated using a sound level calibrator (Bruel & Kjaer, 4231). Recordings were sampled at either 512 kHz or 1 MHz.

In addition to broadband stimuli, the tympana were also stimulated with 4-cycle pulses at 23 kHz (50 Hz burst rate), produced by a function generator (Agilent 33120A, Agilent Technologies UK Ltd., Edinburgh, UK) synchronized with the LDV. The microphone was carefully positioned near the measured tympanum until the phase of the microphone signal and that of the tympanum displacement matched. Tympanal vibrations were recorded from both anterior and posterior tympanal membrane (ATM and PTM, respectively). The instantaneous phase of the stimuli and responses was calculated using Hilbert transform to identify any discrepancy in phase between both signals.

2) Specimens were mounted on a custom-built platform, which provides acoustic isolation between the two main sound inputs of the bush-cricket ear (see figure 1 and supplementary information for details).

Sound was delivered locally at the spiracle and at the tympanum [5] using a custom build probe loudspeaker (figure 1b, see [13] for details). The combination of the probe loudspeaker offering high acoustic impedance and the platform's front panel as an acoustic barrier was sufficient to effectively attenuate high-frequency sound and allow for focal acoustic stimulation.

Using this setup, tympanal vibrations in response to broadband chirps (5-50 kHz) and 23 kHz 4-cycle tones broadcast by the probe loudspeaker at the spiracle were recorded from both ATM and PTM using LDV. The spectrum of the output of the probe loudspeaker was mathematically flattened using the B&K microphone as a reference placed 2 mm away from the probe tip ([13]). We calculated the FFT of the transfer function between the stimulus and tympanal response to obtain the phase spectrum.

2.4. The transmission gains of the trachea

We calculated AT gain (as in [5]) from broadband stimulation, and from time domain recordings using 4-cycle pure-tones at specified frequencies. The response of the tympanum to both types of stimuli was measured using a focal sound source [5, 24] delivering sound at the external surface of the tympanum while isolating the tracheal input (figure 1*b*), and using a probe loudspeaker delivering sound at the acoustic spiracle only (figure 1*c*). For broadband stimulation, we adjusted the sound pressure of the output at 0.02 Pa (~60 dB SPL) as measured at 2 mm away from the probe's tip. We then positioned the probe loudspeaker either at 2 mm away from ATM or PTM, or at 2 mm away from the spiracle. Tracheal gain was quantified as the difference in tympanal displacement (using LDV) between external and tracheal stimulation.

2.5. Statistics and analysis

We compared differences in log tympanal tuning, tracheal time delays between tympana, across individuals, and between sexes using a restricted maximum likelihood linear mixed-effects model (LMM) in R (v.3.2.1, [31]) using the *lmer*Test package [32]. For a detailed description, see supplementary materials.

3. RESULTS

3.1. Anatomical measurements of acoustic trachea

The geometry of the tracheal system was studied using μ-CT, while also evaluating tracheal length using an inserted human hair. The reconstructed 3D models of the acoustic trachea do not reveal sexual dimorphism in their general appearance. However, as an effect of body size, tracheal tubes are slightly, although not statistically significantly, longer in females: females (17.239± 0.724 mm, n=22 [11 left and 11 right]), males (16.272 ± 0.7412 mm: LMM: t=-3.07, d.f.=2.87, p=0.058). Levine test (F=0.05, P=0.956) shows that the variability in left and right measurements between males and females is statistically not significantly different. There was no significant

difference between right and left trachea on its own (t=0.45, d.f.=2.84, p=0.685) or in interaction with sex (t=0.37, d.f.=2.84, p=0.735).

Tracheal morphology in *C. gorgonensis* is typical for conocephaloid bush-crickets [2, 8, 29]. The oval spiracle opens into an ovoid tracheal atrium, the acoustic bulla (figure 2*a, b, c*). Past the bulla, the trachea narrows quickly into a thin tube (figure 2*b, c, d*). Using 3D µ-CT models, we measured the internal AT radii at 25 µm intervals for both left and right tracheae in 2 males and 1 female *C. gorgonensis*. The radius of the trachea varies along its length, progressively narrowing in the first half of its length, after which it stays relatively constant until approaching the ear (figure 2*c, e, f*). The mean radii for left and right tracheae ranged from 169 µm to 185 µm (with SD ranging from 72 µm to 90 µm), while the median values lay between 138 µm and 151 µm (see figure 2*e, f* and supplementary material table S-1).

3.2. Frequency and time domain responses of the tympanal membrane in acoustic free field conditions

Specimens were tethered in the acoustic isolation holder and the vibrational responses of tympana to broadband sound chirps from the ipsilateral side were recorded with the LDV. In all cases, the response frequency spectrum of both tympanal membranes was broad across the measured range. However, both tympanal membranes vibrate with higher amplitudes to frequencies around the frequency of the call (~23 kHz, figure 3*a, b*). Measurement quality and reliability for each measurement point was high as estimated using magnitude-squared coherence [30], in particular for frequencies around 23 kHz (Figure 3*c, d*). There was no difference between frequency tuning (at maximum spectral response) between ATM and PTM across all specimens (LMM: t=-0.81, df=20, p=0.4305). There was, however, a significant negative relationship between tympanal tuning and tracheal length (LMM: t=-2.73, d.f=17, p=0.014), and a trend for this pattern to sex (LMM: t=2.06, d.f=17, P= 0.055). Similarly, there were no significant differences in the tuning of the tympanal membranes between males and females (LMM: t=-2.06, df=17, p=0.055, females=22.92 kHz ± 4.18 kHz, n=22; males 24.41 kHz ± 3.874 kHz, n=20). On average, across all specimens, both tympanal membranes showed best response at 23.63 kHz ± 4.06 kHz, n=42, (figure 3*a, b*).

Recordings of tympanal membrane vibrations were also obtained in the time domain. For these experiments, the specimens were mounted as above, and the loudspeaker placed at 30 cm ipsilateral and perpendicular to the body axis delivering 23 kHz 4-cycle tones at a constant sound pressure of 1 Pa. These experiments were designed to provide direct evidence of the pressure difference system, evaluating the ratios of the magnitudes of the sound pressures acting on the internal and external surfaces of the tympanum. Tympanal vibrations are generated by sound acting from the inner and outer sides of the tympana (figure 4). LDV recordings show that the tympanal vibration is composed of two parts, a segment of low amplitude, and a subsequent part

with high amplitude (figure 4*e*). The low amplitude oscillations represent the free field sound waves acting directly on the external surface of the tympanal membrane (black segment, figure 4*e*), while the high amplitude oscillations are the response to sound waves travelling from the acoustic spiracle via the AT and acting on the internal surface of the membrane (red segment). The latter response betrays the presence of sound waves pushing the membrane in a direction opposite to that exerted by sound acting externally. Hence, this mechanical response is the result of sound acting externally in addition to the vibrations produced by sound acting internally. The exact moment of collision between the two oscillations was identified applying Hilbert transformation to the tympanal displacement to compute the phase information in the time domain [33]. Because the microphone was carefully adjusted as to have the same vertical axis as the tympanal membrane of interest, both the recorded stimulus and the vibration of the tympanal membrane exhibited similar phase during the first sound cycles (figure 4*d, e* and *f*). Some short time after stimulus onset, a clear change in phase of the mechanical response is observed (figure 4*e, f*, asterisk and orange dashed arrow). This phase change indicates the arrival of sound at the internal side of the tympanal membrane (see supplementary material, Video 1). After this moment, the phase of the displacement stays constant in relation to that of the stimulus until the phase difference amounts to ca. 200° (figure 4*f*). Because sound propagation inside the trachea is delayed, the first cycle of the stimulus signal, in phase with initial tympanal vibration (black trace 1 and 2 in figure 4*e*), takes 62-80 µs to strike the tympanal membrane on the internal surface. Thus, the signal arrives at the tympanal membranes twice, with the second arrival delayed by tens of microseconds (figure 4*f*, orange dashed line). In specimens measured within a free sound field (without the sound isolation platform), the time delay varies with distance and azimuth of the sound source in relation to the spiracle and the position of the ear. Cycles of tympanal vibrations corresponding to the external sound arrival are nearly 6 times (5.53 ± 1.35, range 3.87-7.72; 14.85 dB, n=21, measured at the ATM only) quieter than their respectively shifted cycles coming from the trachea (figure 4*e*). These findings highlight the role the acoustic bulla and trachea play in sound amplification, in this case enhancing gain by nearly 15 dB.

3.3. Velocity of sound propagation in the trachea calculated from the frequency and time domains

3.3.1 Calculations in the frequency domain

Periodic chirps in the range of 1-50 kHz were delivered to the spiracle using a calibrated probe loudspeaker continuously monitored with a reference microphone. Acoustic phase at the spiracle and subsequently at the tympanal membrane was evaluated in response to stimulation at the spiracle. In general, phase changes linearly with frequency (figure 5). In the low frequency range (5-10 kHz), the phase at the tympanal membrane changes slowly (by less than half a cycle ~120°) with respect to the phase at the spiracle. This shows that low frequency sound propagates in the trachea with minor impediment. In contrast, at 23 kHz phase changes by nearly 500° (460°-490° in

figure 5*a*, *b*, male and female), revealing a phase shift of nearly 1.3-1.4 cycles. At 23 kHz, such shift corresponds to a time delay of approximately 60 µs. At 40 kHz, the phase change is about 840°-860°, or 2.3-2.4 cycles, also corresponding to approximately 60 µs duration. Calculations in the low frequency range, such as 10 kHz, concur and show that sound propagation time is around 58 to 60 µs.

This analysis therefore suggests that sound velocity inside the trachea remains constant across the frequency range measured.

3.3.2 Calculations in the time domain

The velocity of sound propagation inside the trachea was established by measuring the time lag between the onset of the stimulus delivered at the spiracle and its time of arrival at the tympanal membrane (figure 5*c, d*). At 23 kHz, we measured a propagation time between 60.60 and 82.00 µs, with a mean of 66.37 ± 4.79 µs (ATM, mean±SD, n=21); and 60.20-81.20 µs, mean of 65.96 ± 4.59 µs (PTM; n=21) (figure 5*c, d*). There is no significant difference in the time of arrival at each tympanum (LMM: t=-0.48, d.f.=17.99. p=0.637). Across specimens, the propagation time calculated was not statistically different from the time lag calculated from the phase spectrum at 23 kHz (LMM: t=-0.93, d.f=18.41, p=0.364). In addition, neither sex (LMM: t=-1.17, d.f=22.53, p=0.254) nor the interaction between sex and time lag were significant (LMM: t=1.19, d.f=18.45, p=0.249). At other frequencies (10, 15, 20, 30, 40 and 50 kHz), the transmission time remains constant (63.50 ± 1.36 µs, n=21, PTM only). Altogether, these results agree with the linear response between phase and frequency described in the previous section (see also figure 5*a, b*).

Using this acoustical information and tracheal dimensions, the velocity of sound propagation was calculated as ~255 m/s and found not to differ between right and left trachea (right= 255.2 m/s ± 18.5 m/s, n=21; left=255.8 m/s ± 14.9 m/s, n= 21; SE= 7.17, LMM: t=-0.51, d.f.=20.09, p=0.616). The overall average velocity of sound propagation in the trachea was 255.5 m/s (n=42). The velocity of sound propagation was slightly, but not significantly, higher in the female tracheae (261.3 ± 7.9 m/s, n=22) than in the male tracheae (249.1 ± 21.1 m/s, n=22; LMM: t=-0.53, d.f.=19.31, p=0.602).

Overall, these results show that sound velocity inside the trachea is reduced in relation to that in free field conditions by a factor of 1.35, and confirms figures obtained from the frequency analysis (section 3.5), as well as early work on other species [4, 5, 27].

3.4. Tracheal gain calculations

Tracheal gain functions were measured using both broadband stimulation and time domain responses to 4-cycle pure-tones. The gain was determined by calculating the difference in tympanal deflection between external and tracheal stimulation. The stimulus was presented using equivalent sound pressures either at the external surface of the tympanum or at the acoustic

spiracle entrance. In response to broadband stimulation, the gain function reveals that most of the gain occurs between 15 and 35 kHz (figure 6). Within this range the gain increases from 4.2 to 10.6 (i.e., 12.5 and 20.5 dB), as measured at the ATM (figure 6). This finding demonstrates that the AT performs amplification of sound pressure across a range of frequencies.

4. Discussion

4.1. The velocity of sound transmission in the acoustic trachea

Sound propagates slower inside the AT (~255 m/s), a velocity comparable to those inferred in field crickets and bush-crickets (~260 m/s) [4, 27]. In field crickets, tracheal conduction was shown to enable directional hearing by imposing resistance to sound propagation with respect to sound acting on the external surface of the tympanal membrane [24, 26, 34]. In bush-crickets, species with large thoracic spiracle and large acoustic bullae, such as *C. gorgonensis* (figure 2) [35], the tracheal signal is amplified within a specific range of frequencies, and also incurs a time lag between sound acting on the external and internal sides of the tympanum [4, 5] (figure 6). Additionally, the size of the auditory spiracle is positively correlated with hearing sensitivity [15, 19, 36]. Functionally, the progressive reduction in AT radius (figure 2) has been proposed to act like an exponential horn that enhances sound pressure at its thin end [2, 7, 14]. Our data support the exponential horn model form earlier work [5], suggesting that in bush-crickets the propagation velocity of sound can be seen as largely independent of frequency and therefore non-dispersive. The mechanism responsible for the reduction of sound propagation velocity remains, however, unknown.

It has been long demonstrated that the velocity of sound in a solid tube is greatly reduced when the tube becomes narrow compared to the wavelength of sound, or frequency increases [37, 38]. Interestingly, the empirical values reported here, although in good accord with earlier results [4, 27], are clearly lower than those predicted from conventional equations for the propagation of sound velocity in narrow tubes.

For comparison, we used the following two different approximations of Kirchhoff's solution on the acoustical propagation velocity v developed by Benade [37] and Zwikker & Kosten [39], respectively:

$$v = c \cdot \left(1 - \frac{1}{r_v\sqrt{2}} - \frac{\gamma - 1}{r_t\sqrt{2}}\right) \quad (1)$$

where c is the sound velocity in free field air (343 m/s), r_v and r_t terms for the viscous and thermal boundary layers (see supplementary material, table S-2) and γ the ratio of specific heats (1.4). Notably, the velocity term can be expressed as

$$v = \frac{c}{Im(\Gamma)} \quad (2)$$

with the propagation constant Γ as

$$\Gamma = \sqrt{\frac{J_0(i^{\frac{3}{2}} r_v)}{J_2(i^{\frac{3}{2}} r_v)}} \cdot \sqrt{\frac{\gamma}{n}} \quad (3)$$

where J_0 and J_2 are Bessel functions of 0-th and 2-nd order and n constitutes a term that approaches 1 for $\gamma \rightarrow 1$ (see supplementary material, table S-2 for more details).

Using both Benade's (Eq. 1, [37]) and Zwikker & Kosten's (Eq. 2 & 3, [39]) approximations with standard values for the properties of air and a median trachea radius of 150 µm at 23 kHz, one finds propagation speeds of 318 m/s and 320 m/s respectively (supplementary material, table S-2). There could be several reasons to account for the discrepancy between the results found here and in the acoustic literature.

Firstly, although the equations of Benade [37] and Zwikker & Kosten [39] include the effects of viscous and thermal boundary layers (r_v and r_t, respectively) within the tube, the general assumption is that of an adiabatic system where no heat is exchanged with the surroundings. Interestingly, Fletcher [40] argues that the adiabatic assumption in narrow tubes is only valid for radial frequencies ω

$$\omega \gg \frac{\pi \kappa}{\alpha^2} \quad (4)$$

where κ is the thermal diffusivity ($\sim 1.9*10^{-5}$ m^2/s) and a the tube radius and $\omega=2\pi f$. Using 23 kHz as frequency f and 150 µm as tube radius in Eq. 4 results in ω being roughly 50 times bigger than the right hand side of Eq. 4. Although Fletcher does not state a definite cut-off value for the transition from isothermal to adiabatic, it is reasonable to assume a rather gradual transition from low-frequency isothermal to high-frequency adiabatic conditions. If so, the system described here could be viewed as isothermal, then a variation of Zwikker & Kosten's equation can be used, where $\gamma=1$ [38], which changes Eq. 3 to:

$$\Gamma = \sqrt{\frac{J_0(i^{\frac{3}{2}} r_v)}{J_2(i^{\frac{3}{2}} r_v)}} \quad (5)$$

Substituting Eq. 5 in Eq. 2 results in a propagation velocity within the tube of 276 m/s, much closer to our experimental values (see also table S-2:.

A second possible explanation for our relatively low propagation speed can be found in the nature of the classical equations underlying the analytical approximations used here. Although basic properties of the medium (like density, viscosity and ratio of specific heats) and dimensions of the tube are taken into account, no terms for the elasticity (like Young's modulus or bulk modulus) and thickness of the tube walls are considered.]nsect tracheae are very thin and quite unlike the rigid structures assumed previously. Considering these additional material properties and others within the system (like internal pressure, changes in composition and humidity of the gas mixture, etc.)

may provide more accurate understanding of isothermal and adiabatic propagation inside sound tracheal systems.

4.2. The tracheal transmission gain

In response to 4-cycle pure-tone stimuli, tympanal membranes undergo vibrations that are, in linear terms, 4-6 times larger for internal sound pressures than for external ones, a response that varies with frequency. Such response gains range from 12 to 16 dB, as calculated from time domain and broadband measurements.

We have shown here that sound pressure amplification is a result of sound travelling inside the gradually narrowing AT. The data reveal that pressure amplification originates from internal sound pathways (figure 4) in *C. gorgonensis*, suggesting that each ear, working as a pressure difference receiver, can independently process directional information. Although not the scope of this study, the reported dependence of tympanal vibrations on the azimuth of sound incidence in other cricket species [22, 24] supports the presence of a similar mechanism in *C. gorgonensis*. Operating at ultrasonic frequencies, however, these ears may also exploit instantaneous phase relationships between the ATM and PTM within a single ear, essentially offering the possibility that each ear is directional. Ultrasonic frequencies such as that of the species calling song may generate diffractive effects around the ears and the tympanal flaps and result in differences in phase of vibration between the tympanal membranes of a single ear [42]. The functional morphology of such ears, potentially exploiting 6 distinct acoustic inputs, remains to be studied in detail, especially questioning the role of tracheal transmission and microacoustical diffraction in the biophysics of auditory directionality.

5. Conclusions

Quantifying the acoustic transmission characteristics of the AT in *C. gorgonensis*, we present direct biophysical measurements of the mechanisms at work in an auditory pressure difference receiver. Both spectral and time-resolved measurements presented here allow for a deeper understanding of this widespread form of auditory system, the pressure-difference receiver.

A pressure difference receiver relies on the interference of sound waves at both surfaces of the tympanal membranes [23-25]. We demonstrate here the existence of two pressure wave fronts -the differential pressure waves- their relative timing and effect of their superposition on tympanal vibrations. Carried out over a broad range of frequencies, the temporal analysis of these two waves demonstrates that sound travels inside the AT at a constant velocity and thus non-dispersively (as found by [27]). This behaviour does not comply with the theoretical frequency dependence of propagation velocities in narrow tubes. This deviation from theory reveals an interesting functional characteristic of this sound transmission system, as it allows for a spectrally broadly tuned system

to reliably transmit finely resolved undistorted temporal and spectral informational content to the ears' receptive structures. Minimal dispersion in effect serves the coherent transfer of the spiracular acoustic input to the internal face of the tympanum where it interacts with the external and original version of itself. Biophysically, it is presumably advantageous for this auditory system to produce interference between signals void of frequency dependent delays of distortions. In this sense, preserving both the spectro-temporal characteristics and temporal patterns of the species-specific narrow-band song may facilitate the delicate frequency decomposition process carried out by the ear of *Copiphora* [13]. It can be argued here that similar demands exist to preserve the coherence of multiple acoustic inputs when they originate from the environment of other signalling species.

It has been suggested that pressure difference receivers operate only at low frequencies and low internal amplifications [43], with the consequence that for higher frequencies and amplification, the system would operate more like a conventional pressure receiver, yet dominated by large internal pressure input [7, 17, 44]. However, such a proposal only considers the actual amplification through tracheal propagation (12-20 dB over the frequency range from 5-50 kHz in this case) and does not take into account the additional level of mechanical amplification that results from the lever-like energy transfer between the tympanum and the tympanal plate [13]. Even minuscule tympanal displacements in response to low amplitude acoustic stimulation produce large deflections of the *crista acustica* surface, comparable or larger than those of the tympanum (but see fig. 5 in Montealegre-Z & Robert [29]). The increased sound pressure produced by tracheal amplification acting on the inner tympanal surface increases this effect and is most likely dependent on wave diffraction at the position of the spiracular opening. In the same way, external sound waves will be diffracted by the animal's cuticular flaps covering the ears that will affect their impact on the vibration of the tympanal membranes.

Since pressure difference receivers are inherently directional due to the differential phase and amplitude components of the two incident sound waves [24], the high amount of amplification generated by the AT suggests that *Copiphora* could use these differential inputs to perform accurate localization of sound sources. If this is indeed the case, the importance of diffraction at both the spiracle and the cuticular ear flaps and the sensitivity of the system to directional signals is currently still unknown.

Authors' contributions. F.M-Z., T.J. and D.R. conceived and designed the experiments. F.M-Z. and T.J. performed the experiments. KR-B performed µCT scans and processed X-ray images for further analysis. F.M-Z, T.J. and C.S. analysed data. C.S. designed all the statistical models. T.J., D.R. and F.M-Z. wrote the manuscript. All authors reviewed the manuscript.

Competing interests. The authors have declared that no competing interests exist.

Funding: The authors are currently sponsored by the Royal Society, and by the Leverhulme Trust (grant No. RPG-2014-284). This research was also sponsored by the Human Frontier Science Program (Cross Disciplinary Fellowship LT00024/2008- C to F.M-Z.) and the BBSRC to D.R.

Acknowledgements. The Colombian Ministry of Environment granted a permit for fieldwork at Gorgona National Park (resolución DTS0-G-31 11/2007, and resolución DTS0-G-090 14 08/2014). All applicable international, national, and/or institutional guidelines for the care and use of animals were followed. We would also like to thank two anonymous reviewers for their constructive comments on the manuscript.

Figure caption

Figure 1. Experimental setup. (*a*) Frontal view of the isolating platform. (*b*) Setup used to stimulate the ear using tracheal input only. The probe loudspeaker is placed at 2 mm away from the spiracle. The LDV records tympanal vibrations, while a microphone positioned at ear location monitors that sound from the probe loudspeaker does not cross the isolating panel. (*c*) Setup used to occlude tracheal input. A sound-attenuating cylinder is assembled at the posterior side of the platform, enclosing the body region containing the spiracle. A microphone is inserted inside the cylinder to monitor sound entering the chamber; a syringe needle allows balancing atmospheric pressure inside. A probe loudspeaker is positioned near the tympanum for external sound delivery.

Figure 2. Anatomy of the acoustic trachea measured using μCT. (*a*) Frontal view of a male *C. gorgonensis* with head, legs and thorax in transparency showing the AT. (*b*) Lateral view of the body in transparency showing left and right AT. (*c*) Close up view of the acoustic spiracle and bulla.
(*d*) Internal view inside the acoustic trachea. (e) and (f) Quantitative relationship between tracheal diameter and length, displayed from the acoustic spiracle to the tympanal organ area in a male and a female, respectively.

Figure 3. Tympanal vibrations in respond to broadband stimulus in free-field conditions, shown as the average spectrum ATM (a) and PTM (b), measured across 21 individuals (10 males and 11 females). (c) Coherence plots of ATM vibration. (d) Coherence plots of PTM vibration

Figure 4. ATM motion in response to free-field pure-tone stimulation. (*a-b*) Orientation image relating ear topography to the position of the scanning lattice. (c) Vibration map of the ATM response measured as displacement. Deflections are shown for different phases along the

oscillation cycles (numbers match the cycles shown in *d* and *e*. Note that the tympanal plate (as described in [13]) is not included in the scan. (*d*) 23 kHz 4-cycle tone played at ca. 1 Pa. (*e*) Tympanal vibrations recorded with LDV. Initial dashed line represents sound arriving at the exterior tympanum surface. The red trace shows tympanal motion with additional internal acoustic tracheal input. (*f*) Phase analysis of tympanal response. The interference between external and internal inputs results in a significant change in phase at 81 µs. This phase shift is also apparent from the change of the otherwise sinusoidal membrane displacement (red asterisk in *e*). The oscillation marked with number 1 in the microphone trace in *d*, and in the laser trace in *e*, corresponds to the oscillation marked with 1* in *e*. (g-i) Average stimulus, response, and instantaneous phase (as shown in panels *d-f*) measured on the left ATM across 11 females.

Figure 5. Tracheal sound propagation, frequency and time domain analysis. (*a*) ATM and PTM response to broadband stimulation for a male and a female. (*b*) Phase spectrum of the response highlighting the phase lag at 23 and 40 kHz. (*c-d*) Vibration of the tympana in response to sound (23 kHz, 4-cycle tone) travelling through the AT only. (*c*) Oscillograms showing the stimulus recorded at the spiracle entrance of a male and a female. (*d*) Mechanical response of both tympanal membranes in the same individuals. The response is notably delayed in each case (shaded areas) in relation to the microphone onset as sound propagates through AT.

Figure 6. Gain measurements across the spectral range. (*a*) ATM response in females (n=11). (*b*) ATM response in males (n=10). Black outline shows the tympanal response to external input only. Red trace shows tympanal response when sound is delivered at the acoustic spiracle and transmitted via the AT only. Shaded areas indicate standard deviation in both cases (n=11 females).

REFERENCES

[1] Heinrich, R., Jatho, M. & Kalmring, K. 1993 Acoustic Transmission Characteristics of the Tympanal Tracheas of Bush-Crickets (Tettigoniidae). 2. Comparative-Studies of the Tracheas of 7 Species. *Journal of the Acoustical Society of America* **93**, 3481-3489.

[2] Hoffmann, E. & Jatho, M. 1995 The Acoustic Trachea of Tettigoniids as an Exponential Horn - Theoretical Calculations and Bioacoustical Measurements. *Journal of the Acoustical Society of America* **98**, 1845-1851.

[3] Kalmring, K. & Jatho, M. 1994 The Effect of Blocking Inputs of the Acoustic Trachea on the Frequency Tuning of Primary Auditory Receptors in 2 Species of Tettigoniids. *Journal of Experimental Zoology* **270**, 360-371.

[4] Larsen, O.N. 1981 Mechanical time resolution in some insect ears. 2. Impulse sound-transmission in acoustic tracheal tubes. *Journal of Comparative Physiology* **143**, 297-304.

[5] Michelsen, A., Heller, K.G., Stumpner, A. & Rohrseitz, K. 1994 A New Biophysical Method to Determine the Gain of the Acoustic Trachea in Bush-Crickets. *Journal of Comparative Physiology A Sensory Neural and Behavioral Physiology* **175**, 145-151.

[6] Rajaraman, K., Mhatre, N., Jain, M., Postles, M., Balakrishnan, R. & Robert, D. 2013 Low-pass filters and differential tympanal tuning in a paleotropical bushcricket with an unusually low frequency call. *Journal of Experimental Biology* **216**, 777-787. (doi:10.1242/jeb.078352).

[7] Shen, J.X. 1993 A peripheral mechanism for auditory directionality in the bush-cricket *Gampsocleis gratiosa* - acoustic tracheal system. *Journal of the Acoustical Society of America* **94**, 1211-1217. (doi:10.1121/1.408174).

[8] Bailey, W.J. 1990 The ear of the bushcriket. In *The Tettigoniidae. Biology, Systematics and Evolution* (eds. W.J. Bailey & D.C.F. Rentz), pp. 217-247. Bathurst, Australia, Crawford House Press.

[9] Rossler, W., Hubschen, A., Schul, J. & Kalmring, K. 1994 Functional-morphology of bush-cricket ears - comparison between 2 species belonging to the Phaneropterinae and Decticinae (Insecta, Ensifera). *Zoomorphology* **114**, 39-46.

[10] Roessler, W., Jatho, M. & Kalmring, K. 2006 The auditory-vibratory sensory system in bushcrickets. In *Insect Sounds and Communication: Physiology, Behaviour, Ecology and Evolution* (eds. S. Drosopoulos & M. Claridge), pp. 35-69. London, Taylor & Francis.

[11] Schumacher, R. 1975 Scanning-Electron-Microscope description of the tibial tympanal organ of the Tettigonioidea (Orthoptera, Ensifera). *Z. Vergl. Physiol.* **81**, 209-219.

[12] Schumacher, R. 1973 Morphologische Untersuchungen der tibialen Tympanalorgane von neun einheimischen Laubheuschrecken-Arten (Orthoptera, Tettigonioidea). *Zeitschrift für Morphologie der Tiere* **75**, 267-282.

[13] Montealegre-Z, F., Jonsson, T., Robson-Brown, K.A., Postles, M. & Robert, D. 2012 Convergent evolution between insect and mammalian audition. *Science* **338**, 968-971.

[14] Lewis, D.B. 1974 The physiology of the tettigoniid ear. I. The implications of the anatomy of the ear to its function in sound reception. *Journal of Experimental Biology* **60**, 821-837.

[15] Nocke, H. 1975 Physical and physiological properties of the tettigoniid ('grasshopper') ear. *Journal of Comparative Physiology* **100**, 25–57.

[16] Stephen, R.O. & Bailey, W.J. 1982 Bioacoustics of the ear of the bushcricket *Hemisaga* (Sagenae). *Journal of the Acoustical Society of America* **72**, 13-25.

[17] Seymour, C., Lewis, B., Larsen, O.N. & Michelsen, A. 1978 Biophysics of the ensiferan ear. *Journal of comparative physiology* **123**, 205-216. (doi:10.1007/bf00656873).

[18] Mason, A.C., Morris, G.K. & Wall, P. 1991 High ultrasonic hearing and tympanal slit function in rainforest Katydids. *Naturwissenschaften* **78**, 365-367.

[19] Bailey, W.J. 1993 The Tettigoniid (Orthoptera, Tettigoniidae) Ear - Multiple Functions and Structural Diversity. *International Journal of Insect Morphology and Embryology* **22**, 185-205.

[20] Morris, G.K., Klimas, D.E. & Nickle, D.A. 1989 Acoustic signals and systematics of false-leaf Katydids from Ecuador (Orthoptera, Tettigoniidae, Pseudophyllinae). *Transactions of the American Entomological Society (Philadelphia)* **114**, 215-263.

[21] Stumpner, A. & Heller, K.-G. 1992 Morphological and physiological differences of the auditory system in three related bushcrickets (Orthoptera: Phaneropteridae,

Poecilimon). *Physiological Entomology* **17**, 73-80. (doi:10.1111/j.1365-3032.1992.tb00992.x).
[22] Michelsen, A. 1979 Insect ears as mechanical systems. *American Scientist* **67**, 697-706.
[23] Robert, D. 2005 Directional hearing in insects. In *Sound Source Localization* (eds. A.N. Popper & R.R. Fay), pp. 6-35. New York, Springer-Verlag
[24] Michelsen, A. & Larsen, O.N. 2008 Pressure difference receiving ears. *Bioinspiration & Biomimetics* **3**. (doi:10.1088/1748-3182/3/1/011001).
[25] Michelsen, A., Popov, A.V. & Lewis, B. 1994 Physics of directional hearing in the cricket *Gryllus bimaculatus*. *Journal of Comparative Physiology a-Sensory Neural and Behavioral Physiology* **175**, 153-164.
[26] Michelsen, A. 1994 Directional hearing in crickets and other small animals. In *Neural Basis of Behavioural Adaptations* (ed. K.E.N. Schildberger), pp. 195-207.
[27] Bangert, M., Kalmring, K., Sickmann, T., Stephen, R., Jatho, M. & Lakes-Harlan, R. 1998 Stimulus transmission in the auditory receptor organs of the foreleg of bushcrickets (Tettigoniidae) I. The role of the tympana. *Hearing Research* **115**, 27-38.
[28] Montealegre-Z, F. & Postles, M. 2010 Resonant sound production in *Copiphora gorgonensis* (Tettigoniidae: Copiphorini), an endemic species from Parque Nacional Natural Gorgona, Colombia. *Journal of Orthoptera Research* **19**, 347-355.
[29] Montealegre-Z, F. & Robert, D. 2015 Biomechanics of hearing in katydids. *J Comp Physiol A* **201**, 5-18. (doi:10.1007/s00359-014-0976-1).
[30] Windmill, J.F.C., Gopfert, M.C. & Robert, D. 2005 Tympanal travelling waves in migratory locusts. *Journal of Experimental Biology* **208**, 157-168.
[31] Team, R.C. 2016 R: A language and environment for statistical computing. (Vienna, Austria, R Foundation for Statistical Computing.
[32] Kuznetsova, A., Brockhoff, P.B. & Christensen, R. 2014 lmerTest: tests in liner mixed effects models. (R package v2.0-20. ed.
[33] Hartmann, W.H. 1998 *Signals, Sound and Sensation*. New York, Springer Verlag.
[34] Michelsen, A. 1998 The tuned cricket. *News in Physiological Sciences* **13**, 32-38.
[35] Bailey, W.J. & Yang, S. 2002 Hearing asymmetry and auditory acuity in the Australian bushcricket *Requena verticalis* (Listroscelidinae; Tettigoniidae; Orthoptera). *Journal of Experimental Biology* **205**, 2935-2942.
[36] Bennet-Clark, H.C. 1984 Insect Hearing: Acoustics and transduction. In *Insect Communication* (ed. T. Lewis), pp. 49-82. London, Academic Press.
[37] Benade, A.H. 1968 On the propagation of sound waves in a cylindrical conduit. *Journal of the Acoustical Society of America* **44**, 616-623.
[38] Tijdeman, H. 1975 On the propagation of sound waves in cylindrical tubes. *Journal of Sound and Vibration* **39**, 1-33.
[39] Zwikker, C. & Kosten, C.W. 1949 *Sound absorbing materials*. New York Elsevier Pub. Co.
[40] Fletcher, N.H. 1974 Adiabatic Assumption for Wave Propagation. *American Journal of Physics* **42**, 487489. (doi:dx.doi.org/10.1119/1.1987757).
[41] Douglas, J., Gasiorek, J., Swaffield, J. & Jack, L. 2005 *Fluid Mechanics*. 5th Edition ed, Pearson Education Limited.
[42] Bailey, W.J. & Stephen, R.O. 1978 Directionality and auditory slit function - Theory of hearing in bushcrickets. *Science* **201**, 633-634. (doi:10.1126/science.201.4356.633).

[43] Michelsen, A. & Larsen, O.N. 1985 Hearing and Sound. In *Comprehensive Insect Physiology Biochemistry and Pharmacology* (eds. G.A. Kerkut & L.I. Gilbert), p. Pergamon. New York, Pergamon.

[44] Michelsen, A. & Larsen, O.N. 1978 Biophysics of the ensiferan ear: I. Tympanal vibrations in bushcriekets (Tettigoniidae) studied with Laser Vibrometry. *Journal of Comparative Physiology A Sensory Neural and Behavioral Physiology* **123**, 193-203.

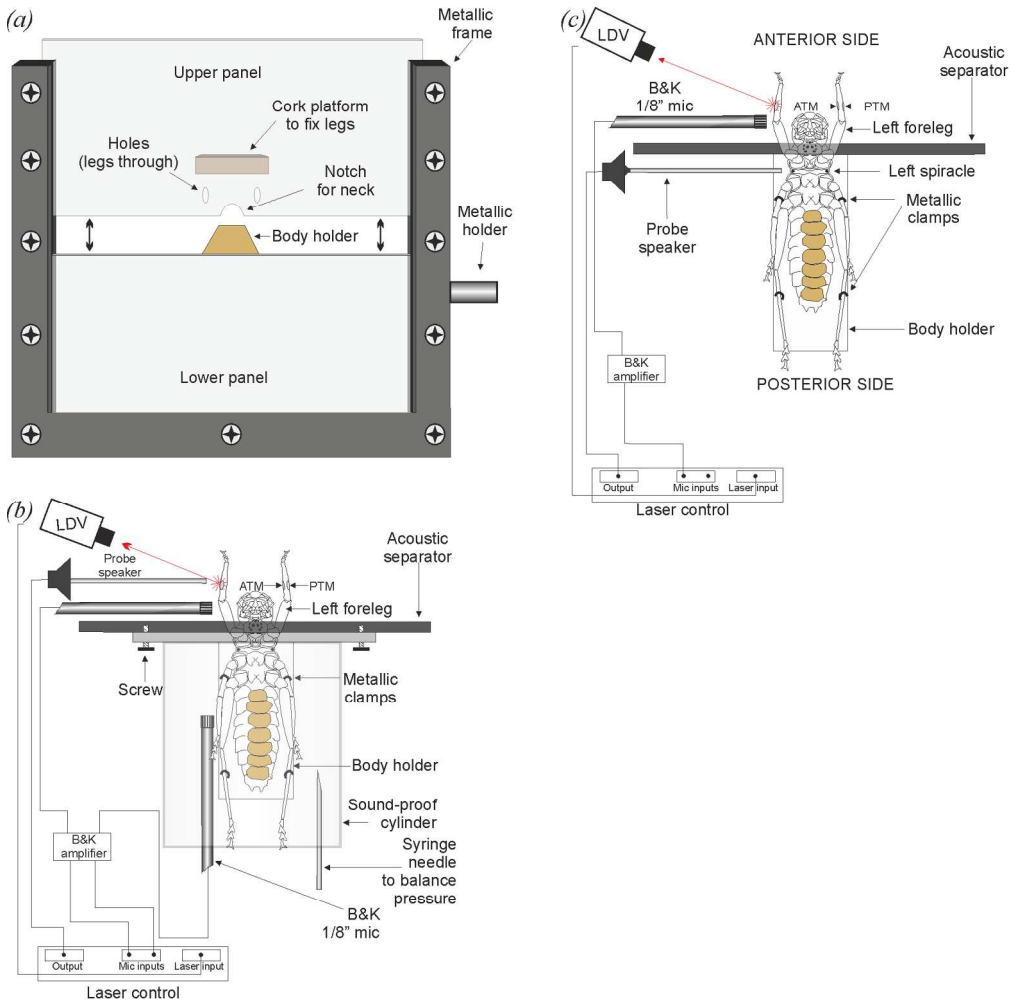

Figure 1. Experimental setup. (a) Frontal view of the isolating platform. (b) Setup used to stimulate the ear using tracheal input only. The probe loudspeaker is placed at 2 mm away from the spiracle. The LDV records tympanal vibrations, while a microphone positioned at ear location monitors that sound from the probe loudspeaker does not cross the isolating panel. (c) Setup used to occlude tracheal input. A sound-attenuating cylinder is assembled at the posterior side of the platform, enclosing the body region containing the spiracle. A microphone is inserted inside the cylinder to monitor sound entering the chamber; a syringe needle allows balancing atmospheric pressure inside. A probe loudspeaker is positioned near the tympanum for external sound delivery.

figure 1

174x172mm (300 x 300 DPI)

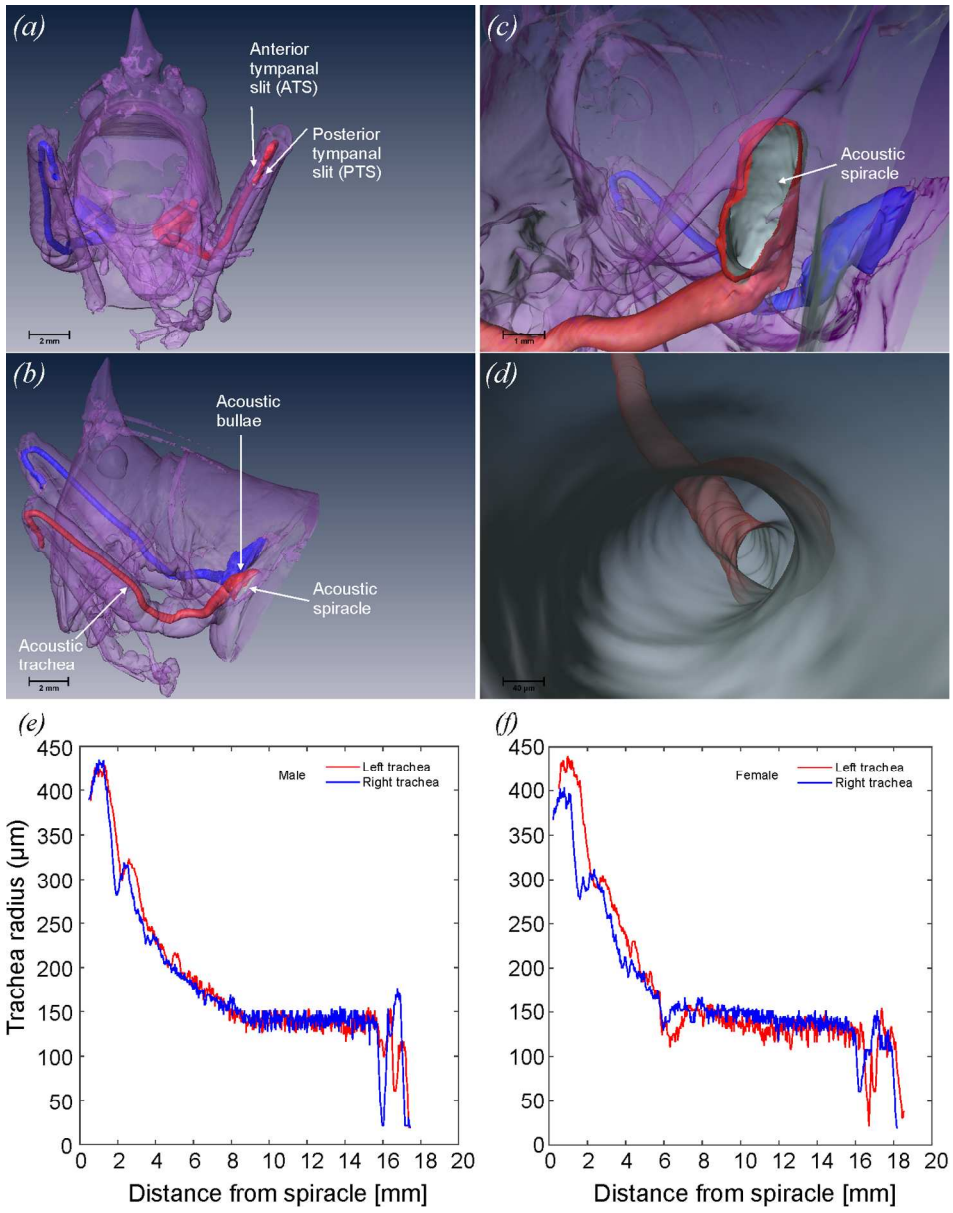

Figure 2. Anatomy of the acoustic trachea measured using *µ*CT. (a) Frontal view of a male *C. gorgonensis* with head, legs and thorax in transparency showing the AT. (b) Lateral view of the body in transparency showing left and right AT. (c) Close up view of the acoustic spiracle and bulla.
(d) Internal view inside the acoustic trachea. (e) and (f) Quantitative relationship between tracheal diameter and length, displayed from the acoustic spiracle to the tympanal organ area in a male and a female, respectively.
figure 2
137x175mm (300 x 300 DPI)

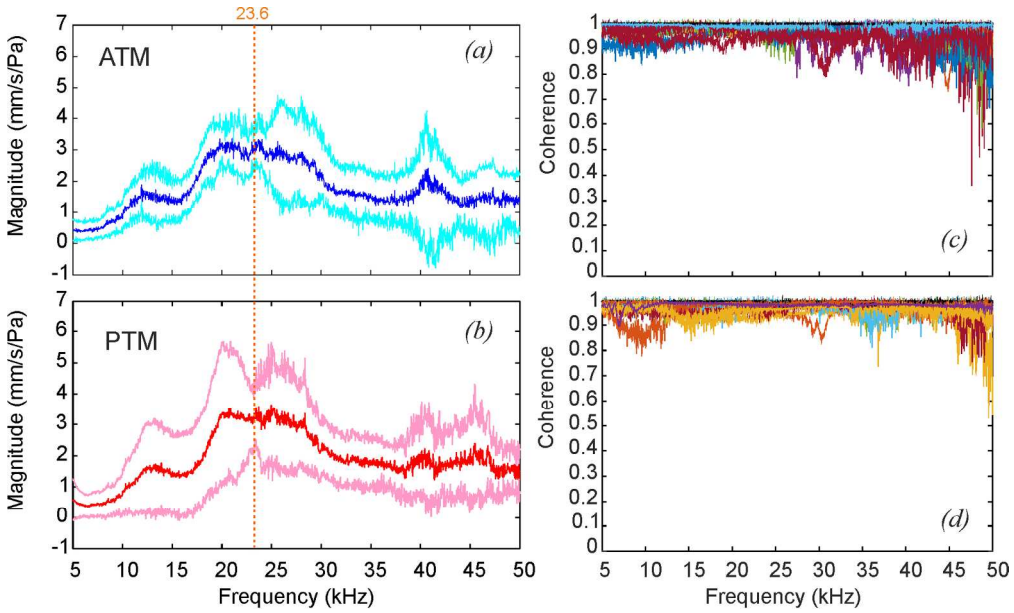

Figure 3. Tympanal vibrations in respond to broadband stimulus in free-field conditions, shown as the average spectrum ATM (a) and PTM (b), measured across 21 individuals (10 males and 11 females). (c) Coherence plots of ATM vibration. (d) Coherence plots of PTM vibration.
figure 3
166x100mm (300 x 300 DPI)

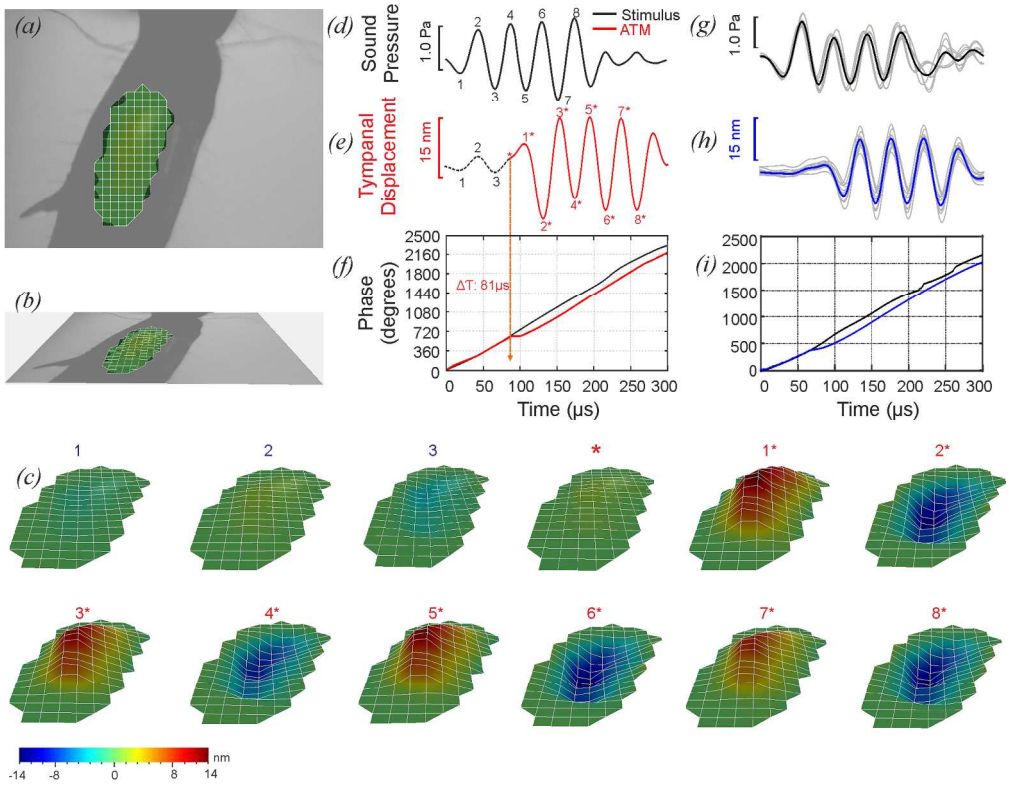

Figure 4. ATM motion in response to free-field pure-tone stimulation. (a-b) Orientation image relating ear topography to the position of the scanning lattice. (c) Vibration map of the ATM response measured as displacement. Deflections are shown for different phases along the oscillation cycles (numbers match the cycles shown in d and e. Note that the tympanal plate (as described in [13]) is not included in the scan. (d) 23 kHz 4-cycle tone played at ca. 1 Pa. (e) Tympanal vibrations recorded with LDV. Initial dashed line represents sound arriving at the exterior tympanum surface. The red trace shows tympanal motion with additional internal acoustic tracheal input. (f) Phase analysis of tympanal response. The interference between external and internal inputs results in a significant change in phase at 81 μs. This phase shift is also apparent from the change of the otherwise sinusoidal membrane displacement (red asterisk in e). The oscillation marked with number 1 in the microphone trace in d, and in the laser trace in e, corresponds to the oscillation marked with 1* in e. (g-i) Average stimulus, response, and instantaneous phase (as shown in panels d-f) measured on the left ATM across 11 females.

figure 4

178x138mm (300 x 300 DPI)

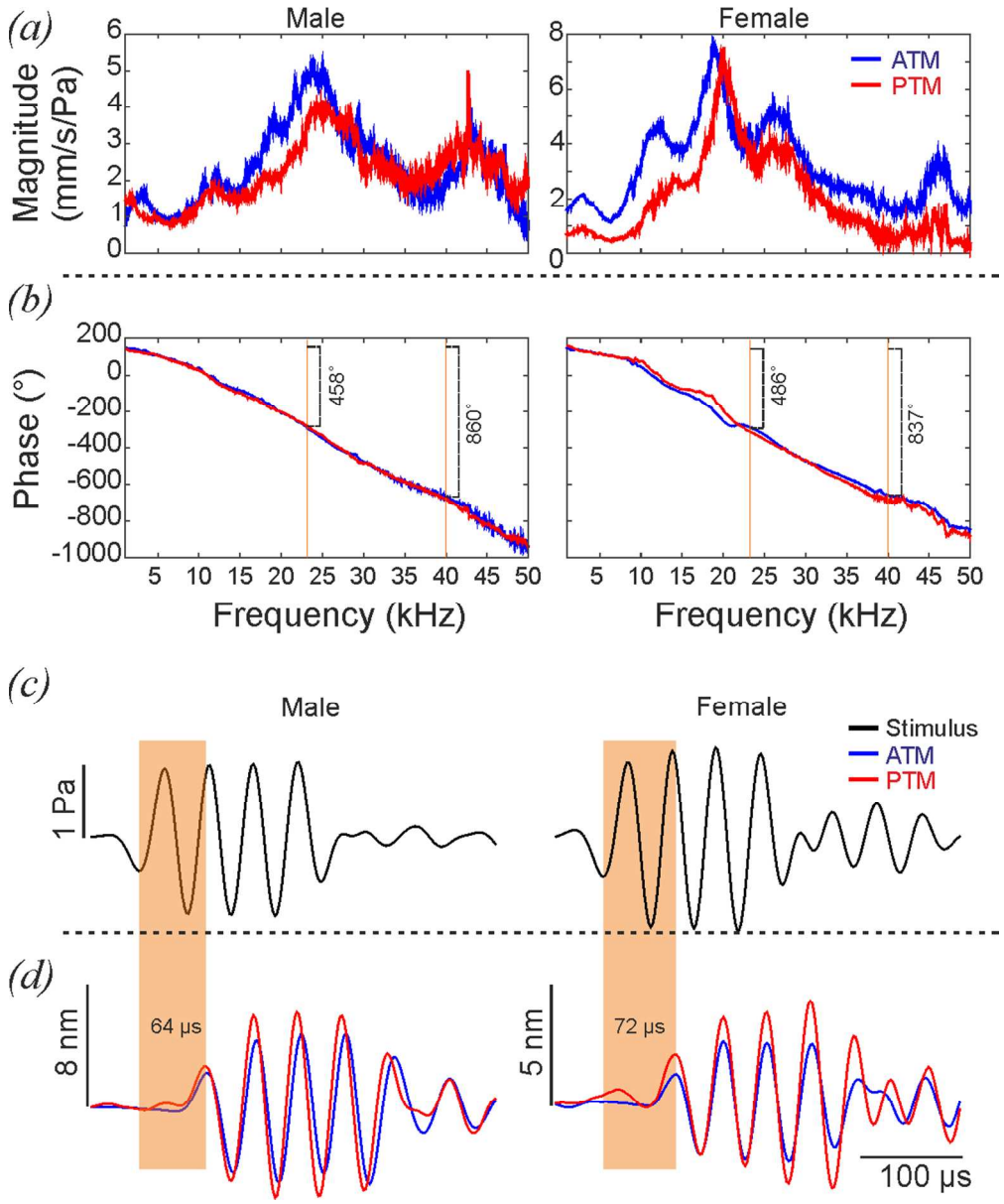

Figure 5. Tracheal sound propagation, frequency and time domain analysis. (a) ATM and PTM response to broadband stimulation for a male and a female. (b) Phase spectrum of the response highlighting the phase lag at 23 and 40 kHz. (c-d) Vibration of the tympana in response to sound (23 kHz, 4-cycle tone) travelling through the AT only. (c) Oscillograms showing the stimulus recorded at the spiracle entrance of a male and a female. (d) Mechanical response of both tympanal membranes in the same individuals. The response is notably delayed in each case (shaded areas) in relation to the microphone onset as sound propagates through AT.

figure 5

101x122mm (300 x 300 DPI)

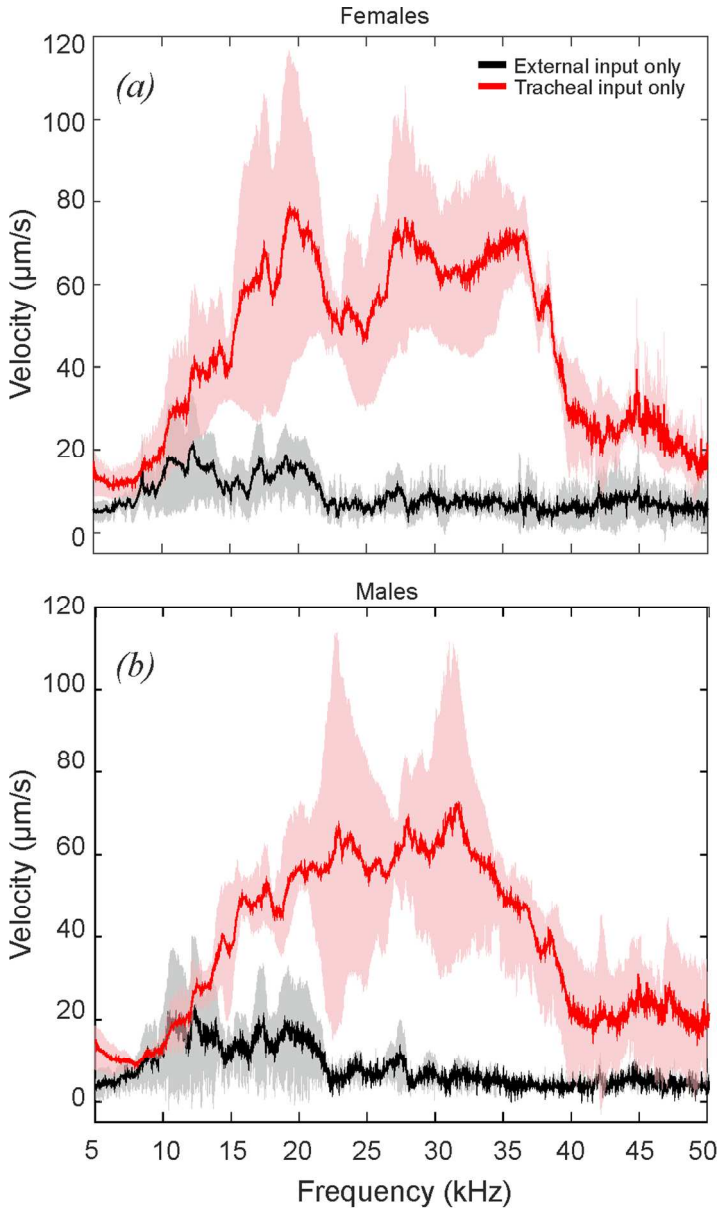

Figure 6. Gain measurements across the spectral range. (a) ATM response in females (n=11). (b) ATM response in males (n=10). Black outline shows the tympanal response to external input only. Red trace shows tympanal response when sound is delivered at the acoustic spiracle and transmitted via the AT only. Shaded areas indicate standard deviation in both cases (n=11 females).
figure 6
85x145mm (300 x 300 DPI)